Increased Rubisco content in maize mitigates chilling stress and speeds recovery

Coralie E. Salesse-Smith[1,2] (iD), Robert E. Sharwood[3] (iD), Florian A. Busch[3] (iD) and David B. Stern[1,2,*] (iD)

[1]*Boyce Thompson Institute, Ithaca, NY, USA*

[2]*Plant Biology Section, School of Integrative Plant Science, Cornell University, Ithaca, NY, USA*

[3]*Research School of Biology, The Australian National University, Canberra, ACT, Australia*

Summary

Many C_4 plants, including maize, perform poorly under chilling conditions. This phenomenon has been linked in part to decreased Rubisco abundance at lower temperatures. An exception to this is chilling-tolerant *Miscanthus,* which is able to maintain Rubisco protein content under such conditions. The goal of this study was to investigate whether increasing Rubisco content in maize could improve performance during or following chilling stress. Here, we demonstrate that transgenic lines overexpressing Rubisco large and small subunits and the Rubisco assembly factor RAF1 (RAF1-LSSS), which have increased Rubisco content and growth under control conditions, maintain increased Rubisco content and growth during chilling stress. RAF1-LSSS plants exhibited 12% higher CO_2 assimilation relative to nontransgenic controls under control growth conditions, and a 17% differential after 2 weeks of chilling stress, although assimilation rates of all genotypes were ~50% lower in chilling conditions. Chlorophyll fluorescence measurements showed RAF1-LSSS and WT plants had similar rates of photochemical quenching during chilling, suggesting Rubisco may not be the primary limiting factor that leads to poor performance in maize under chilling conditions. In contrast, RAF1-LSSS had improved photochemical quenching before and after chilling stress, suggesting that increased Rubisco may help plants recover faster from chilling conditions. Relatively increased leaf area, dry weight and plant height observed before chilling in RAF1-LSSS were also maintained during chilling. Together, these results demonstrate that an increase in Rubisco content allows maize plants to better cope with chilling stress and also improves their subsequent recovery, yet additional modifications are required to engineer chilling tolerance in maize.

Introduction

Zea mays (maize) is one of the world's most important food crops, with 14.6 billion bushels (approximately 370 million metric tons) produced in the United States in 2017. Although maize is tropical in origin, more than 60% of its production occurs in countries with temperate climates (Ranum *et al.*, 2014). The United States is the world's largest producer, with the majority of production in the Midwest where the growing season averages 4–5 months due to temperature limitations. Sensitivity to chilling conditions has long been a concern for maize cultivation, even as climate change has encouraged earlier planting, paradoxically increasing the risk of exposure to chilling conditions. Improving the ability of maize to tolerate cooler conditions could broaden the latitudes at which maize can be grown, and lengthen the growing season and productivity where it is grown already (Dohleman and Long, 2009).

C_4 plants such as maize are commonly more efficient than C_3 plants in their use of light, nitrogen and water (Long, 1983). This is in part due to their ability to concentrate CO_2 in bundle sheath (BS) cells and avoid the energetic cost of photorespiration, even with the additional energy required to fix CO_2 twice in the C_4 dicarboxylate cycle. Under chilling conditions, however, C_4 plants generally

perform poorly relative to their C_3 counterparts. One hypothesis is that photorespiration in C_3 plants decreases with decreasing temperature, thereby reducing the net energy expended per CO_2 molecule fixed under cooler conditions (Ehleringer and Björkman, 1977; Osborne *et al.*, 2007), whereas at 25 °C, the energy expended per CO_2 molecule fixed is approximately equal in C_3 and C_4 plants (Ehleringer and Björkman, 1977). This observation, combined with the geographical distribution of C_4 plants, led to the suggestion that C_4 plants may be competitively excluded from colder climates. Additional evidence suggests that the C_4 pathway arose multiple times in different C_3 species in tropical and subtropical regions in response to low CO_2 atmospheres and/or stress conditions such as heat, drought and high light (Sage *et al.*, 2012). This evolutionary history may help explain why many C_4 plants perform poorly under cooler conditions.

Another factor that has been hypothesized to contribute to the poor performance of C_4 plants under chilling conditions is that they possess 60%–80% less Rubisco on a total protein basis than C_3 plants (Long, 1999; Sage *et al.*, 1987). This predisposes them to Rubisco limitations in cool conditions where turnover rates are slowed, and Rubisco catalysis cannot keep pace with RuBP regeneration and CO_2 levels (Sage, 2002). A study that used antisense transgenic technology to reduce Rubisco abundance in

C_4 *Flaveria bidentis* found that Rubisco accounts for up to 70% of the light-saturated photosynthesis (A_{SAT}) limitation at optimal temperatures, and is likely to become more limiting (~99%) at suboptimal temperatures (Kubien *et al.*, 2003).

Not all C_4 plants are chilling sensitive, however. The best-studied example is *Miscanthus × giganteus*, a perennial C_4 energy crop. *Miscanthus* is considered chilling tolerant due to its ability to maintain photosynthetically active leaves at 14 °C (Beale *et al.*, 1996; Naidu and Long, 2004). *Miscanthus* has also been to shown to maintain photochemical quenching (q_P), maximum quantum yield of photosystem II (Φ_{PSII}), CO_2 assimilation and the expression of rate-limiting enzymes under chilling conditions (Farage *et al.*, 2005; Long and Spence, 2013; Wang, Portis, *et al.*, 2008). In addition, comparative transcriptomics showed up-regulation of several photosynthetic genes in response to chilling (Spence *et al.*, 2014).

In contrast to *Miscanthus*, chilling-sensitive plants such as maize are unable to maintain photosynthetically efficient leaves under chilling temperatures. In maize, the capacity for carbon assimilation can decrease over 60% (Long and Spence, 2013), accompanied by decreases in q_P, Φ_{PSII} and in total leaf Rubisco and pyruvate phosphate dikinase (PPDK) protein content (Long, 1983; Wang, Naidu, *et al.*, 2008). This is due to a combination of chilling-dependent photoinhibition and impaired synthesis of PSII and light-harvesting complex proteins, which results in nonfunctional PSII reaction centres (Fryer *et al.*, 1995; Long *et al.*, 1994). Additionally, numerous enzyme activities are reduced under chilling temperatures, photosynthetic genes are down-regulated, and protein stability and solubility are altered (Ruelland *et al.*, 2009; Spence *et al.*, 2014). Increased accumulation of Rubisco breakdown products upon cold stress suggests that the enzyme becomes unstable (Kingston-Smith et al., 1999). The same study also showed significant decreases in Rubisco activity during chilling, even though the enzyme was fully activated. In maize, Rubisco content has been shown to decrease by ~40%, while it is maintained in chilling-tolerant C_4 species, implying the maintenance of Rubisco may be important for maintaining photosynthetic capacity at low temperatures (Long and Spence, 2013; Naidu *et al.*, 2003; Wang, Naidu, *et al.*, 2008).

We hypothesized that normally chilling-sensitive maize could compensate for cooler temperatures by producing more Rubisco compared to other leaf photosynthetic enzymes during acclimation to chilling, or by having adequate Rubisco prestress to avoid limitation at low temperatures. Thus, increasing Rubisco content in maize could theoretically provide a means to enhance chilling tolerance. Our previous work documented a >30% increase in maize Rubisco content conditioned by transgenic overexpression of the Rubisco large (LS) and small subunits (SS) with Rubisco Assembly Factor 1 (RAF; Salesse-Smith *et al.*, 2018). The current study examines the properties of these transgenic lines during chilling and recovery to better understand Rubisco's limitation on C_4 photosynthesis during chilling stress, and to ascertain whether increased Rubisco content confers a metabolic advantage under such conditions.

Results

Transgenic lines with increased Rubisco content maintain their growth advantage under chilling conditions

Three previously reported transgenic lines were used in the experiments here: UBI-RAF1, UBI-LSSS and UBI-RAF1-LSSS (Salesse-Smith *et al.*, 2018; Wostrikoff *et al.*, 2012). These lines express RAF1 and/or the Rubisco large and small subunits (LSSS), driven by the highly expressed maize ubiquitin promoter. The LS transgene is a nuclear codon-optimized version flanked by a Flag epitope tag, whose product is efficiently assembled into Rubisco alongside LS produced from the endogenous chloroplast *rbcL* gene. Because transformation had been carried out in the Hi-II genetic background, untransformed Hi-II plants were used as WT controls.

To explore whether increased Rubisco content can improve plant performance under chilling conditions, we germinated plants at 25 °C and grew them for 3 weeks, before exposing them to 14 °C for 2 weeks followed by 1 week of recovery at 25 °C, in keeping with previously published protocols (Spence *et al.*, 2014; Wang, Naidu, *et al.*, 2008). It was visually obvious that LSSS and RAF1-LSSS were larger after chilling than WT or RAF1 (Figure 1a). To quantify this observation, we measured plant height, above-ground fresh and dry weight and leaf area before and during chilling stress, and after recovery. These data revealed significant increases in RAF1-LSSS relative to WT for each growth parameter measured (Figures 1b-d and S1a). LSSS exhibited increased height, fresh and dry weight but not leaf area under chilling stress conditions.

The increases observed for RAF1-LSSS and LSSS are either due to increased growth before chilling, during chilling or both. To determine which scenario is most likely, we used the data in Figures 1d and S1b to calculate the per cent change in plant height and area of the youngest fully developed leaf for each genotype relative to WT, before (3 weeks old) and after (5 weeks old) chilling. We found that RAF1-LSSS and LSSS were 32%–35% taller than WT both before and after chilling stress, indicating that the benefit of increased Rubisco content on plant height largely occurs under control conditions. Similarly, measurements of leaf area showed that LSSS maintains a 39% increase in the area of the youngest fully developed leaf compared to WT between the beginning and the end of the chilling treatment. In contrast, RAF1-LSSS had a 63% larger leaf area than WT before chilling and increased this advantage to 76% after chilling. These results indicate that RAF1-LSSS is capable of increased growth relative to WT in terms of leaf area both under control conditions and throughout chilling conditions, while increases in leaf area for LSSS occur during control conditions. Additionally, we observed that increases in height and leaf area were dramatically slowed in all genotypes in response to chilling stress, as expected, but resumed after temperatures were returned to 25 °C (Figures 1d and S1b). In contrast, plant growth in terms of stalk diameter was not strongly affected by chilling stress (Figure S1c).

The CO_2 assimilation rate is increased in RAF1-LSSS during chilling stress

To investigate whether increased growth of LSSS and RAF1-LSSS during chilling is associated with increased photosynthesis, CO_2 assimilation (A) was measured in response to intercellular CO_2 concentration (C_i) at three time points: prestress (control), after 2 weeks at 14 °C (chilling stress) and after one week of recovery at 25 °C. CO_2 assimilation rates of RAF1-LSSS and LSSS plants trended higher at C_i > 150 µL/L under each condition measured (Figure 2a-c). At light-saturated photosynthetic capacity (A_{SAT}), RAF1-LSSS exhibited a significant, 12% increase in CO_2 assimilation under control conditions, and was 17% higher than the control after 2 weeks at 14 °C (Figure 2d-e). This is in line with
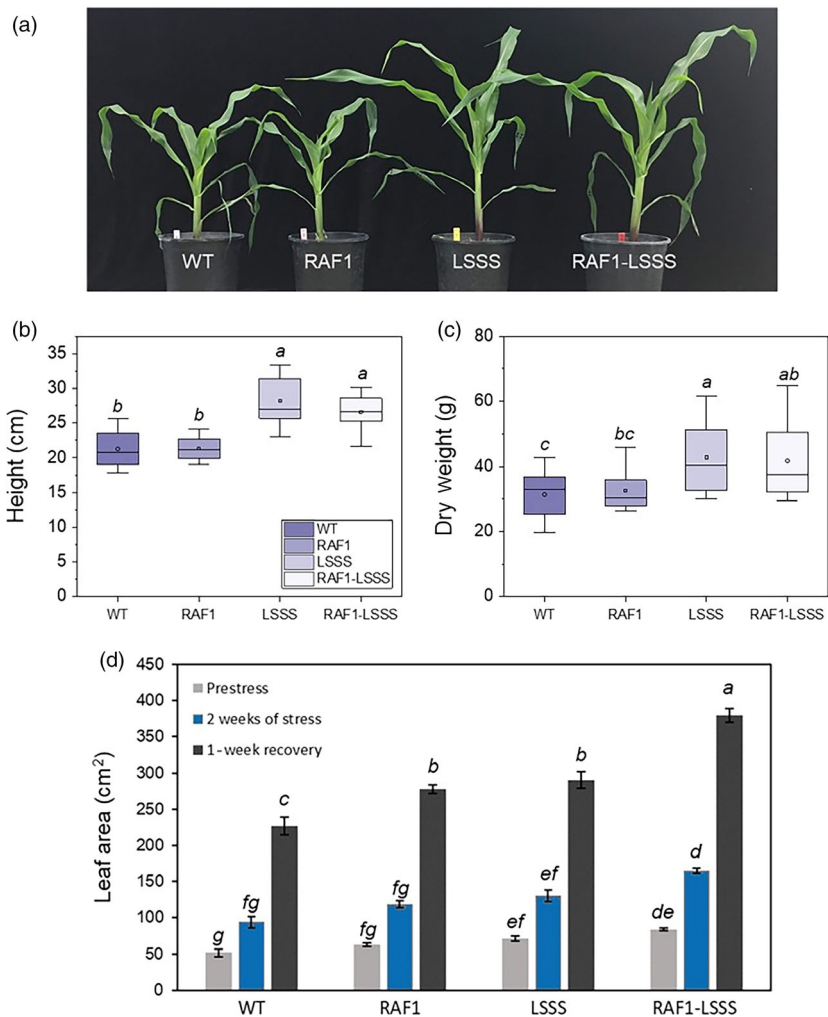
Figure 1 Growth analysis of 3- to 5-week-old plants grown at 14 °C followed by 1 week at 25 °C. (a) A representative plant for each genotype is pictured after 2 weeks of chilling (5 weeks old). (b) Plant height and (c) above-ground dry weight measured after recovery (6 weeks old). n = 12–14 plants per genotype. In each box plot, the black square indicates the mean and the horizontal bar indicates the median. The lower and upper edge of each box indicates the interquartile (25%–75%) range of the values reported. The whiskers extend to 1.5 times the interquartile range. (d) Area of the youngest fully expanded leaf measured at the end of the indicated conditions. n = 5–7 plants per genotype. Values are shown as the mean $\pm$ standard error. Different lowercase letters indicate significant differences ($P < 0.05$), one-way ANOVA Tukey HSD.

our previous observation that CO_2 assimilation increased in RAF1-LSSS by 15% under control conditions, relative to WT plants (Salesse-Smith *et al.*, 2018). Compared to control conditions, however, photosynthetic rates decreased by approximately 50% in response to chilling in all genotypes (Figure 2e), consistent with published results (Long and Spence, 2013). After 1 week of recovery, photosynthetic rates increased substantially, but remained slightly lower than prestress levels (Figure 2f). Together, these results suggest that the additional CO_2 being fixed in RAF1-LSSS and LSSS is contributing to the increased growth seen during chilling stress. For plants grown at higher light (600 vs. 400 μmol/m²/s), A/Ci curves measured during chilling stress exhibited even larger increases (~30%) in photosynthetic rates relative to WT (Figure S2).

Next, we focused on the response of CO_2 assimilation rates to low intercellular CO_2 concentrations (<50 μL/L), to gain insight on PEPC carboxylation efficiency during chilling stress. The initial slope of the A/Ci curves reflects the carboxylation efficiency of assimilation, which in C_4 plants is thought to be strongly influenced by the *in vivo* activity of PEPC (von Caemmerer, 2000). It should be considered, however, that the slope may additionally reflect carbonic anhydrase activities, as well as CO_2 diffusion between cells (mesophyll conductance and BS leakiness). Under control conditions, PEPC carboxylation efficiency was similar between all genotypes (Figure 3a and c), in keeping with our prior observation that all genotypes had similar PEPC

activity (Salesse-Smith *et al.*, 2018). During chilling stress, carboxylation efficiency decreased significantly in all genotypes, except for RAF1-LSSS where only a minimal decrease was observed (Figure 3b-c). Figure 3d shows that exposure to chilling results in the initial slope decreasing approximately 25% in RAF1-LSSS compared to 50% in the remaining genotypes. These results suggest that PEPC activity is not limiting CO_2 assimilation in RAF1-LSSS during chilling stress and that increased Rubisco may be coupled with an increase in initial slope due to the close coupling of the C_3 and C_4 cycles.

RAF1-LSSS plants have improved recovery from chilling stress

Chilling stress has been associated with PSII damage in maize as well as in other chilling-sensitive species (Andrews *et al.*, 1995; Smillie and Hetherington, 1983), which can be detected by measuring chlorophyll fluorescence. We hypothesized that genotypes with increased photosynthetic rates would be able to better protect PSII from damage because a greater proportion of light energy would be allocated to productive photochemistry. To test this, we first measured the potential quenching efficiency of the plants using pulse amplitude fluorometry. We partitioned the excitation energy into Φ_{PSII}, Φ_{CI}, Φ_{REG} and $\Phi_{f,CON}$ according to Busch *et al.* (2009) in order to interpret the relative potential contribution of different processes to energy dissipation and
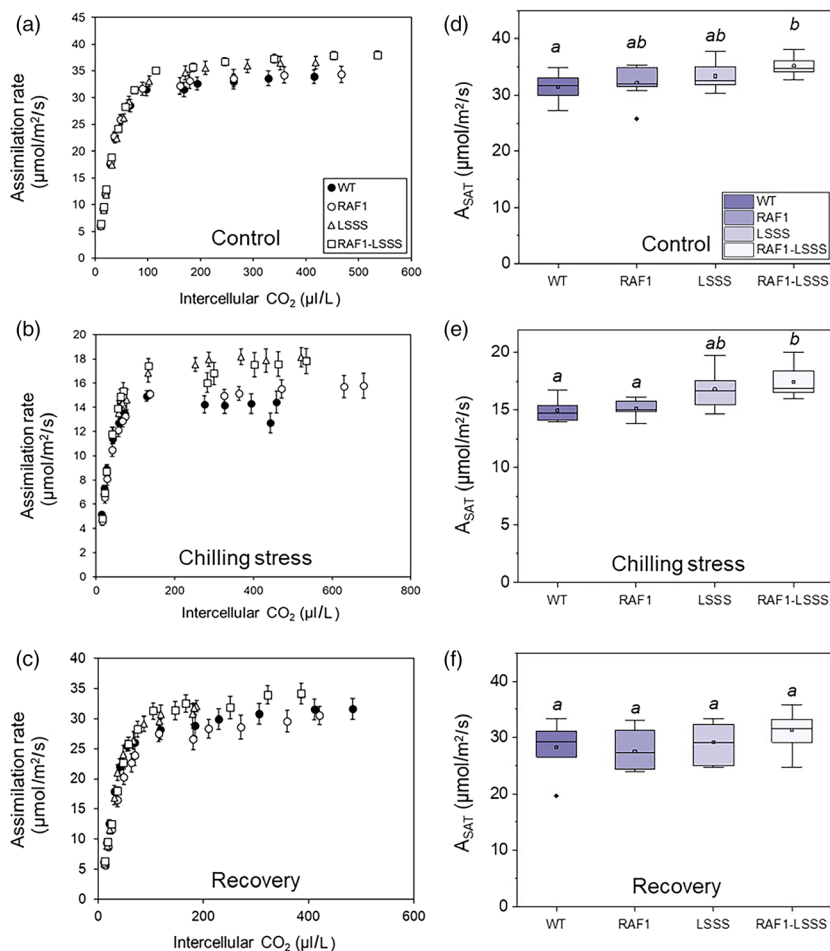
Figure 2 CO_2 assimilation. Response of assimilation rates to intercellular CO_2 concentration measured on the youngest fully expanded leaves of (a) 3-week-old plants before chilling (control); (b) 5-week-old plants at the end of 2 weeks of chilling; and (c) 6-week-old plants after one-week recovery. Maximum light-saturated rate of photosynthesis (A_{SAT}) measured (d) before, (e) during and (f) after chilling. Plants were grown at a light intensity of 350–400 µmol/m^2/s. In each box plot, the black square indicates the mean and the horizontal bar indicates the median. The lower and upper edge of each box indicates the interquartile (25%–75%) range of the values reported. The whiskers extend to 1.5 times the interquartile range, and the black points represent outliers. Measurements were made on 6–9 plants of each genotype at a photon flux density of 1800 µmol/m^2/s. A_{SAT} measurements were performed at a CO_2 concentration of 400 µL/L. Different lowercase letters indicate significant differences ($P < 0.05$), one-way ANOVA Tukey HSD.

utilization in the light-adapted state (Figure 4a). Here, Φ_{PSII} represents the potential quantum efficiency of PSII electron transfer. Φ_{CI} represents the quantum efficiency of nonphotochemical quenching due to sustained photoinhibition by photoinactivated PSII reaction centres during chilling and recovery conditions. Φ_{REG} represents the quantum efficiency of reversible nonphotochemical quenching by active reaction centres, and $\Phi_{f,CON}$ represents the quantum efficiency of fluorescence and constitutive thermal dissipation. Under control conditions, both RAF1-LSSS and LSSS showed significant increases in Φ_{PSII} relative to WT, at the cost of Φ_{REG}, indicating increased potential for electron transport. When exposed to chilling stress, Φ_{PSII} decreased in all lines, while Φ_{CI} and Φ_{REG} increased correspondingly. These results show that chilling conditions limit the potential quantum yield of PSII and promote nonphotochemical energy dissipation across all genotypes. However, we also observed that RAF1-LSSS plants undergo the least amount of photoinhibition during chilling stress, while LSSS undergo the most photoinhibition (Figure 4a). During recovery, RAF1-LSSS showed the largest improvement of Φ_{PSII}, while in the other genotypes Φ_{PSII} remained relatively stable. This indicates that the RAF1-LSSS plants are able to recover from the chilling stress faster than all other genotypes. Throughout the experiment, all genotypes showed similar levels of light dissipation via fluorescence and heat, as measured by $\Phi_{f,CON}$.

Next, we measured Φ_{II} and 1-q_L to look at effective quantum efficiencies. Φ_{II}, the effective quantum yield of linear electron transport, was significantly higher than WT in both LSSS and RAF1-LSSS under control conditions. Φ_{II} values of all plants decreased under chilling conditions, while only RAF1-LSSS showed a significant increase in Φ_{II} during the recovery stage (Figure 4b). 1-q_L, the excitation pressure of PSII, was similar in all genotypes during control and chilling conditions (Figure 4c). Excitation pressure increased in response to chilling, indicating a weaker sink for electrons in the Calvin–Benson cycle. During recovery, a moderate decrease in excitation pressure was observed, with the most prominent decrease occurring in RAF1-LSSS (Figure 4c), suggesting an increase in the electron sink capacity.

Lastly, we measured F_v/F_m and the nonphotochemical quenching parameter *NPQ*. The maximum quantum efficiency of PSII reaction centres (F_v/F_m) represents the fraction of absorbed photons used for photochemistry in a dark-adapted leaf and is a good indicator of PSII integrity. Figure S3a shows no significant differences in F_v/F_m prior to chilling stress, while F_v/F_m decreased significantly in all genotypes except for RAF1-LSSS in response to chilling, with LSSS being the most strongly affected. After being returned to 25 °C for 1 week, F_v/F_m of all genotypes recovered to near prestress levels. *NPQ* is a measure of the reversible nonphotochemical quenching relative to the sustained thermal dissipation. In the control condition, RAF1-LSSS plants had significantly lower values of *NPQ* than WT. During chilling, only RAF1-LSSS experienced an increase in *NPQ* along with a stable F_v/F_m (Figure S3) and relatively low Φ_{CI} (Figure 4a), which together
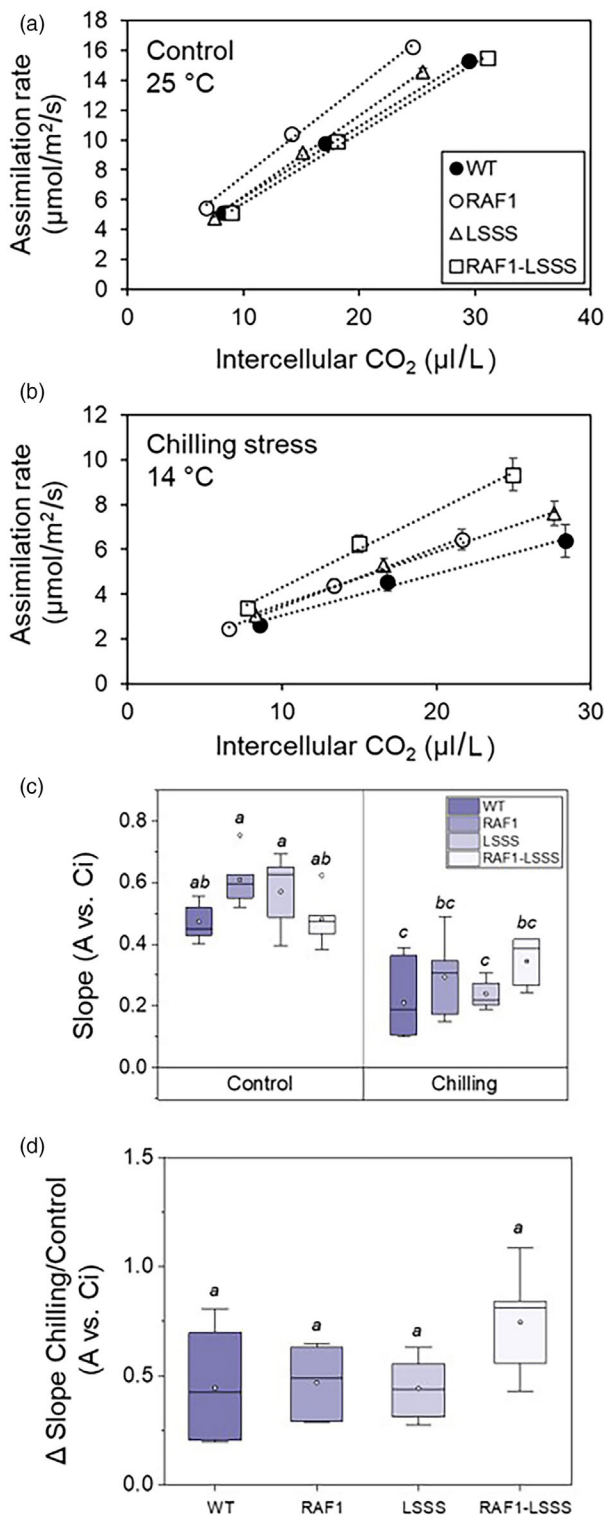
(a)

(b)

(c)

(d)

Figure 3 Response of CO_2 assimilation rates to low intercellular CO_2 concentrations. Gas exchange was performed on the youngest fully expanded leaves of (a) 3-week-old plants before chilling stress (control) and (b) 5-week-old plants at the end of 2 weeks of chilling stress. Plants were grown at a light intensity of 600 $\mu mol/m^2/s$. Values are shown as the mean ± standard error. Measurements were made on 5–8 plants of each genotype at a photon flux density of 1800 $\mu mol/m^2/s$. (c) Box plots of the slope of each genotype under chilling and control conditions calculated using linear regression analysis and (d) the corresponding change between slopes after exposure to chilling conditions. In each box plot, the black square indicates the mean and the horizontal bar indicates the median. The lower and upper edge of each box indicates the interquartile (25%–75%) range of the values reported. The whiskers extend to 1.5 times the interquartile range and the black points represent outliers. Different lowercase letters indicate significant differences ($P < 0.05$), one-way ANOVA Tukey HSD. In panel (c), the ANOVA is done across both growth conditions to observe changes across conditions as well as between genotypes.

in the large decrease of 1-q_L in this line (Figure 4c). In contrast, in all other lines the recovery of electron sink capacity lags behind that of PSII, indicated by the large increase in NPQ during the recovery period (Figure S3b). Taken together with the chlorophyll fluorescence measurements, we conclude that of the genotypes with increased photosynthesis, only RAF1-LSSS plants (which have increased amounts of Rubisco) were able to better protect PSII, while PSII of LSSS plants was most damaged during the chilling treatment. Additionally, RAF1-LSSS was the only genotype that showed multiple measurable signs of improvement at the recovery time, indicative of faster recovery from chilling stress.

RAF1-LSSS maintains the differential increase in Rubisco content relative to WT during chilling

We next evaluated whether increased photosynthetic rates during chilling were correlated with increased Rubisco content, as assayed by ^{14}C-CABP binding. LSSS and RAF1-LSSS possessed significantly more Rubisco than RAF1 ($P < 0.05$; Figure 5a), and RAF1-LSSS Rubisco content exceeded that of WT at $P < 0.1$. Regression analysis showed a correlation between Rubisco content and light-saturated photosynthetic capacity (A_{SAT}), where $P = 0.17$ ($R^2 = 0.68$, Figure 5b). We then measured the Rubisco activation state, which is the proportion of Rubisco reaction sites that are catalytically active, and no significant differences were observed (Figure 5c). This agrees with previous work that suggests Rubisco activase is not limiting under chilling conditions in maize (Kingston-Smith et al., 1999). We then used these measurements to calculate in vitro V_{CMAX} (% active Rubisco × Rubisco content × k_{cat}). A k_{cat} of 5.5 s^{-1} was used based on experimental measurements for maize (Sharwood et al., 2016). These values revealed increases in the amount of active Rubisco in transgenic lines overexpressing the Rubisco subunits, though not significant at $P < 0.05$ (Table 1). In addition, we measured the maximal carboxylation activity of Rubisco using an NADH-linked spectrophotometric assay, to help compare with physiological measurements of CO_2 assimilation. We also measured PEPC activity in vitro using the same method, to see how the results compared to the in vivo measurements. RAF1 showed significant decreases in both Rubisco and PEPC activities, while no differences were seen in the other transgenic lines relative to WT

indicates that in this transgenic line chilling-induced photoinhibition is low compared to the other lines and excess energy is dissipated mostly in regulated, dark-reversible processes rather than associated with sustained PSII inactivation. While NPQ increased considerably during recovery in all other lines, NPQ values in RAF1-LSSS plants remained stable. This shows that only in RAF1-LSSS the recovery of electron sink capacity of the Calvin–Benson cycle keeps pace with PSII recovery, which is also reflected
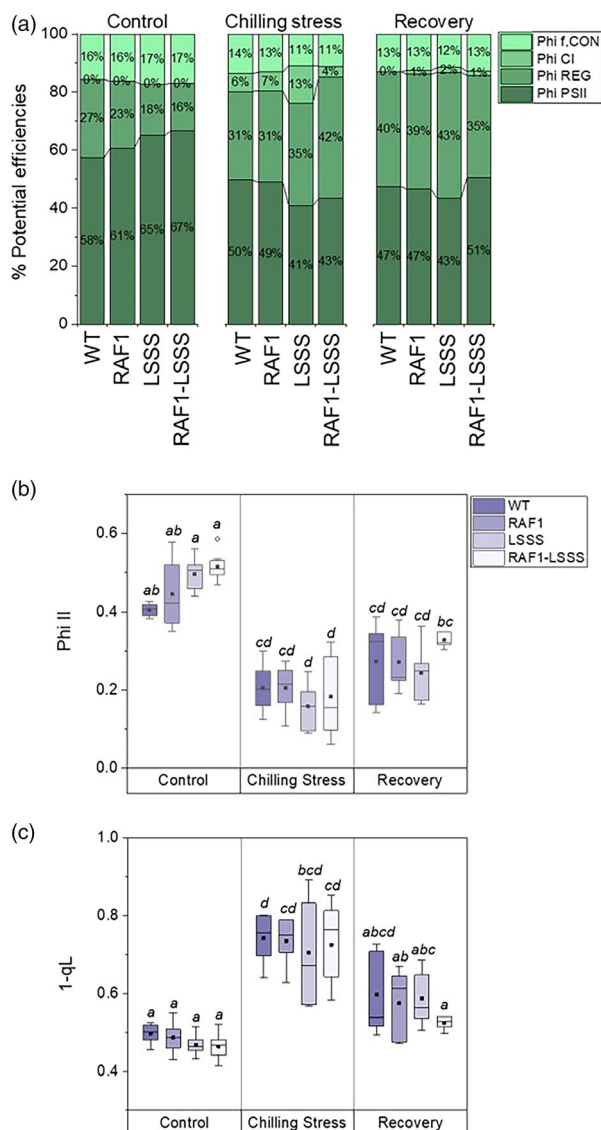
Figure 4 Potential and operative energy quenching efficiencies. (a) Per cent potential quenching efficiency measured as the combination of Φ_{PSII}, Φ_{CI}, Φ_{REG} and $\Phi_{f,CON}$. (b) Maximum quantum efficiency of photosystem II reaction centres (Phi II) and (c) the excitation pressure of photosystem II (1-q_L). Chlorophyll fluorescence measurements were made on the youngest fully developed leaf of 6–9 plants at the following time points; 3-week-old plants prestress (control), 5-week-old plants after 2 weeks of chilling stress, and 6-week-old plants after one week of recovery. In each box plot, the black square indicates the mean and the horizontal bar indicates the median. The lower and upper edge of each box indicates the interquartile (25%–75%) range of the values reported. The whiskers extend to 1.5 times the interquartile range and the black points represent outliers. Different lowercase letters indicate significant differences ($P < 0.05$), one-way ANOVA Tukey HSD. The ANOVA is done across the three growth conditions.

(Table 1). These results indicate that overexpression of RAF1 alone is not beneficial and may be detrimental under chilling conditions. The *in vitro* PEPC activity measurements did not agree with the *in vivo* measurements under chilling conditions, which may be related to the complexities of using gas exchange techniques to infer *in vivo* PEPC activity or may be because the *in vitro*

measurements were performed at 25 °C and perhaps does not reflect the proportion of PEPC active under chilling. In addition, we observed Rubisco activity levels measured by the NADH-linked spectrophotometric method did not show the same trend as Rubisco content or *in vitro* V_{CMAX} between the genotypes, as would be expected when activation state is not altered. These results may be an effect of the method used, which has been shown to underestimate Rubisco k_{cat} (Sharwood *et al.*, 2016). An additional source of error could be due to enzyme activity measurements performed at 25 °C, with tissue isolated at 14 °C.

The effect of chilling on soluble protein content was also examined by immunoblot (Figure S4). LS, PEPC and RAF1 protein levels were generally unchanged in all genotypes in response to chilling stress, while malic enzyme (ME) abundance increased. Small increases in PPDK were also observed in response to chilling, along with possible degradation products. These results differ from previous reports where both LS and PPDK content decreased significantly in response to chilling (Long and Spence, 2013; Wang, Portis, *et al.*, 2008). Perhaps these differences can be attributed to the chilling sensitivities of the maize inbred or hybrid lines used in each study, and/or the severity of the imposed stress. For example, in this study plants were grown at a light intensity of 350–400 µmol/m^2/s, while the previous studies were carried out at 500 µmol/m^2/s, conditions where photoinhibition and therefore protein degradation are more likely.

Negative effects of chilling stress early in development on growth and flowering time are not observed in plants with increased Rubisco

In the field, chilling stress is most often encountered early in development. To probe possible effects of early chilling stress on fully grown plants, we followed growth chamber chilling and recovery with transfer to the greenhouse and growth to maturity. A set of control plants, which did not undergo chilling stress, were grown in parallel. Ear leaf area decreased slightly by nonsignificant amounts in all genotypes exposed to early chilling stress, although ear leaf areas for LSSS and RAF1-LSSS that experienced stress nonetheless remained larger than those of WT plants grown without chilling (Figure 6a). Maximum light-saturated photosynthetic rates (A_{SAT}) of the ear leaf at silking remained higher in RAF1-LSSS relative to WT under control conditions, as previously observed (Figure 6b; Salesse-Smith *et al.*, 2018). A general decrease in A_{SAT} was observed between control plants and those that had experienced chilling, which we hypothesized might be due to the age difference of the plants during flowering (see below).

To quantify the effect of early chilling on growth, we measured plant height weekly (Figure S5). Immediately after chilling stress (5 weeks old), all genotypes showed a 52%–53% decrease in height gain relative to control conditions. At week seven, however, 2 weeks after chilling has ceased, significant delays in growth relative to the control can be observed. At 8 weeks, the decrease in height gain was 38% in LSSS plants and only 25% in RAF1-LSSS plants, indicative of different rates of recovery after chilling stress. WT exhibited a significant decrease in final plant height when exposed to early chilling, while the other genotypes were not significantly affected (Figure 6c). Finally, flowering time was measured as days to anthesis, days to silking and the anthesis-silking interval (ASI). Increases in ASI commonly occur in response to stress and have previously been shown to correlate with decreases in yield (Edmeades *et al.*, 2000). All genotypes
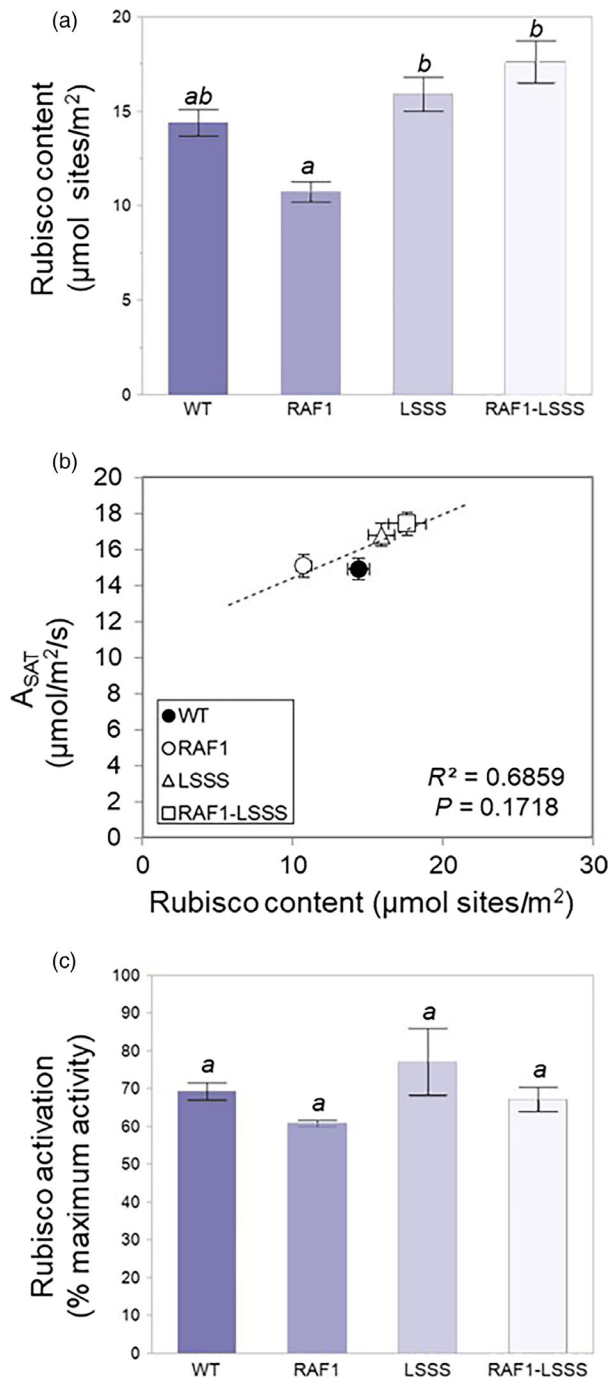
Figure 5 Analysis of Rubisco protein content, activation and enzyme carboxylation activities of 5-week-old plants after 2 weeks of chilling stress. (a) Rubisco content measured by ^{14}C-CABP binding, (b) Rubisco activation status (initial Rubisco activity/total Rubisco activity*100), (c) Rubisco (d) and PEPC activities measured using NADH-linked spectrophotometer assays. Values are shown as the mean ± standard error. Measurements were made on 3–12 plants per genotype. Different lowercase letters indicate significant differences ($P < 0.05$), one-way ANOVA Tukey HSD.

experienced an approximately 10-day delay in anthesis and silking when exposed to 2 weeks' chilling early in development. In addition, both WT and RAF1 showed significant increases in ASI after chilling stress compared to their respective ASI's under

control conditions, indicative of stress and reduction in photo-synthate production during flowering (Figure 6d). Days to anthesis and silking were reduced in RAF1-LSSS during chilling and control conditions when compared to WT plants (Table 2). In general, chilling stress early in development appeared to have the most negative effect on fully grown (reproductive developmental stage) WT plants and the smallest effect on fully grown RAF1-LSSS plants.

Short-term heat stress has similar effects on WT and transgenic plants

We wished to compare effects of chilling to those of heat stress, an abiotic stress condition where Rubisco content is not thought to be the limiting factor in photosynthesis of C$_4$ plants, and where the transgenes could even represent a detrimental genetic load. To do so, 2-week-old plants were placed in 40 °C days and 34 °C nights for 48 h, before measuring photosynthetic rates and collecting leaf tissue. Light-saturated photosynthetic rates decreased significantly in response to heat stress; however, no differences were observed between WT and transgenic plants (Figure S6a). In addition, no obvious phenotypic changes were observed between the genotypes in response to heat stress, apart from their pre-existing size differential (Figure S6b). Protein content of photosynthetic enzymes appeared to be little affected, with the exception of small decreases in Rubisco activase (RCA) in all the lines except RAF1-LSSS (Figure S6c). Those differences were quantified in Figure S6d. Overall, the transgenic lines did not appear to have an advantage or disadvantage compared to WT plants under heat stress, although decreases in RCA abundance could impinge on Rubisco activation, because RCA activity is highly sensitive to thermal denaturation which leads to the deactivation of Rubisco (Salvucci et al., 2001).

Discussion

In this study, we examined whether increased Rubisco content can help mitigate effects of chilling stress on photosynthesis and growth in maize, using a range of transgenic lines already shown to vary in photosynthesis, growth and Rubisco content under control conditions (Salesse-Smith et al., 2018). Here, we recapit-ulated the respective phenotypes prior to exposure to chilling (Figures 1 and 2). The line with increased Rubisco content (RAF1-LSSS), however, maintained a higher photosynthetic rate during chilling stress, with faster recovery and reduced damage to PSII when compared to the other genotypes (Figures 2, 4 and S3). RAF1-LSSS also exhibited increased leaf area, height and dry weight after chilling stress, likely due to the growth advantage the plants had before being exposed to chilling (Figure 1). Thus, increased Rubisco appears to buffer this line against chilling. During the 2-week chilling period, photosynthetic rates were strongly reduced in all genotypes, leading to slowed growth (Figures 1 and 2). This effect is well documented in maize and is due to a variety of factors (Long and Spence, 2013).

One question we aimed to address was whether the low CO$_2$ assimilation rates observed in maize under chilling conditions is a consequence of temperature-induced photoinhibition, or the higher degree of observed photoinhibition is a result from temperature-induced decrease in the electron sink capacity of the Calvin–Benson cycle. The general increase in 1-q_L during the chilling treatment (Figure 4c), which corresponds to an increase in the reduction state of the electron carrier plastoquinone, indicates that the electron sink capacity is more strongly inhibited

Table 1 Summary of leaf gas exchange, chlorophyll fluorescence, plant growth and photosynthetic enzyme activity

Parameter		WT	RAF1	LSSS	RAF1-LSSS	Sample number (*N*)
Leaf gas exchange and chlorophyll fluorescence						
A_{SAT} (μmol/m²/s)	Prestress	31.4 ± 0.9 a	32.1 ± 1.0 ab	33.3 ± 0.9 ab	**35.2 ± 0.6 b**	9
	2 weeks of chilling	14.9 ± 0.4 a	15.1 ± 0.3 a	16.8 ± 0.7 ab	**17.4 ± 0.6 b**	6
F_v/F_m	Prestress	0.785 ± 0.0022 b	0.788 ± 0.0011 ab	0.790 ± 0.0020 ab	**0.797 ± 0.0043 a**	8
	2 weeks of chilling	0.716 ± 0.0072 ab	0.713 ± 0.017 ab	0.632 ± 0.037 b	**0.746 ± 0.0075 a**	6-7
Phi PSII	Prestress	0.405 ± 0.0057 c	0.445 ± 0.030 bc	**0.497 ± 0.014 ab**	**0.516 ± 0.012 a**	8
	2 weeks of chilling	0.206 ± 0.027 a	0.205 ± 0.024 a	0.159 ± 0.021 a	0.184 ± 0.037 a	6-7
NPQ	Prestress	0.941 ± 0.030 c	0.824 ± 0.11 bc	**0.631 ± 0.060 ab**	**0.564 ± 0.035 a**	8
	2 weeks of chilling	0.819 ± 0.083 b	0.798 ± 0.076 b	0.888 ± 0.13 b	**1.25 ± 0.065 a**	6-7
Growth traits						
Height (cm)	2 weeks of chilling	21.3 ± 0.77 b	21.3 ± 0.43 b	**28.2 ± 0.91 a**	**26.6 ± 0.68 a**	12-14
Fresh weight (g)	2 weeks of chilling	123.4 ± 9.4 b	136.8 ± 5.2 b	**177.7 ± 4.6 a**	**168.1 ± 7.0 a**	12-14
Dry weight (g)	2 weeks of chilling	31.4 ± 2.1 c	32.5 ± 1.6 bc	**42.7 ± 3.0 a**	**41.7 ± 3.2 ab**	12-14
Leaf Area of youngest fully developed leaf (cm²)	2 weeks of chilling	93.9 ± 7.7 c	**118.8 ± 4.7 b**	**130.4 ± 7.5 b**	**164.9 ± 3.4 a**	5-7
Photosynthetic enzymes						
Rubisco Content (μmol sites/m²)	2 weeks of chilling	14.4 ± 0.7 ab	10.7 ± 0.5 a	15.9 ± 0.9 b	17.6 ± 1.1 b	3-12
% Rubisco Activation	2 weeks of chilling	69.3 ± 2.3 a	60.8 ± 0.8 a	77.1 ± 8.8 a	67.2 ± 3.2 a	3-5
in vitro V_{cmax} (μmol/m²/s)	2 weeks of chilling	62.8 ± 3.3 a	35.8 ± 1.3 a	63.9 ± 9.4 a	68.3 ± 8.7 a	3-5
Rubisco activity (μmol/m²/s)	2 weeks of chilling	73.3 ± 2.4 a	**43.6 ± 3.0 b**	73.3 ± 6.9 ab	65.7 ± 4.3 a	3-10
PEPC activity (μmol/m²/s)	2 weeks of chilling	222.4 ± 9.1 a	**102.7 ± 14.0 b**	221.1 ± 18.2 a	228.7 ± 14.3 a	3-10

Prestress measurements were taken on 3-week-old plants and 2 weeks of chilling measurements were taken on 5-week-old plants. Data represent averages ± SE. Statistical significance tests were conducted using one-way Tukey–Kramer HSD ANOVA. Values followed by the same letter are not significantly different at *P* < 0.05. Values significantly different from WT at *P* < 0.05 are in bold.

than PSII activity. From this, we conclude that low CO_2 assimilation rates are not caused by photoinhibition of PSII, but that the reason resides in decreased Calvin–Benson cycle activity, in line with previous work (Long *et al.*, 1994). However, during the chilling treatment, the Rubisco overexpressing lines RAF1-LSSS and LSSS did not show higher values of Φ_{II} or Φ_{PSII} (Figure 4a and b), which would be expected if the maintenance of Rubisco during chilling conditions was the main factor limiting CO_2 assimilation. Instead, these results suggest under chilling conditions photosynthesis in maize plants may be sink-limited, resulting in the inability to fully utilize the available photochemical energy through feedback onto Rubisco carboxylation capacity. A detailed comparison of several chlorophyll fluorescence parameters including F_v/F_m and *NPQ* (Figure S3) showed that while the overexpression of Rubisco in RAF1-LSSS plants does not increase photosynthetic electron transport rate *per se*, it did seem to prevent excessive photoinhibition during chilling (relatively low values of Φ_{CI}; Figure 4a) and to facilitate the speedy recovery of photosynthetic capacity upon transfer to the recovery treatment.

We observed that the photosynthetic light reactions recover fairly quickly from chilling stress, with both F_v/F_m and Φ_{CI} recovering almost completely after 1 week (Figures S3a and 4a). In contrast, the photosynthetic carbon fixation reactions are still suppressed, as shown by low levels of photochemical utilization of light energy (Φ_{II}) and high NPQ measured at the recovery time point (Figure 4b and S3b). One possible explanation is that it is easier for PSII to move out of a quenched state than it is for Rubisco and other proteins that decrease during chilling to replenish back to prechilling levels and/or activities. One exception to this pattern was RAF1-LSSS, which had lower NPQ during recovery accompanied by higher Φ_{II} and a 1-q_L value that had almost returned to prechilling levels, though these changes were

not found to be significantly different. This result suggests that during recovery, RAF1-LSSS is able to use more absorbed light energy for photochemistry due to restored balance between the light-dependent and light-independent reactions (Figure 4a and b), implying that increased Rubisco content may in fact help plants recover faster from chilling rather than improve performance during chilling. However, during chilling stress a significant increase in NPQ was observed only in RAF1-LSSS (Figures S3b). This suggests that RAF1-LSSS could be mitigating chilling-induced photoinhibition through the induction of photoprotection (Maxwell and Johnson, 2000). After stress conditions have ceased, a gradual decline in NPQ is expected, which is hypothesized to be related to an increase in CO_2 fixation and deactivation of thermal energy dissipation (Munekage *et al.*, 2002; Murchie and Lawson, 2013). Accelerated recovery from photoprotection or NPQ relaxation has been shown to increase photosynthetic efficiency (Kromdijk *et al.*, 2016). Monitoring NPQ later into the recovery stage might reveal whether RAF1-LSSS plants, where NPQ is induced more rapidly, also have faster relaxation and thus potential for increased photosynthetic efficiency postchilling.

Our experiments have directly tested the hypothesis that photosynthetic assimilation could be improved during chilling by increasing Rubisco content (Friesen and Sage, 2016; Long and Spence, 2013), relative to the broad negative effects that chilling invariably imposes on warm-climate plants (Allen and Ort, 2001). Relative to the WT, RAF1-LSSS CO_2 assimilation is higher by 17% during chilling as compared to 12% in control conditions, in support of this hypothesis. Superimposing high light where the importance of Rubisco is further augmented, an additional relative increase in CO_2 assimilation of ~30% was observed (Figure S2). These results paint a different picture than the chlorophyll fluorescence data, which imply that total Rubisco

Figure 6 Growth analysis of full-grown plants (reproductive developmental stage) exposed to chilling stress early in development. (a) Ear leaf area, (b) maximum light-saturated rate of photosynthesis, (c) height and (d) anthesis-silking interval (ASI) measured on 9–11 plants of each genotype. Chilling stress plants were placed at 14 °C from 3 to 5 weeks of age. In each box plot, the black square indicates the mean and the horizontal bar indicates the median. The lower and upper edge of each box indicates the interquartile (25%–75%) range of the values reported. The whiskers extend to 1.5 times the interquartile range, and the black points represent outliers. Different lowercase letters indicate significant differences ($P < 0.05$), one-way ANOVA Tukey HSD.
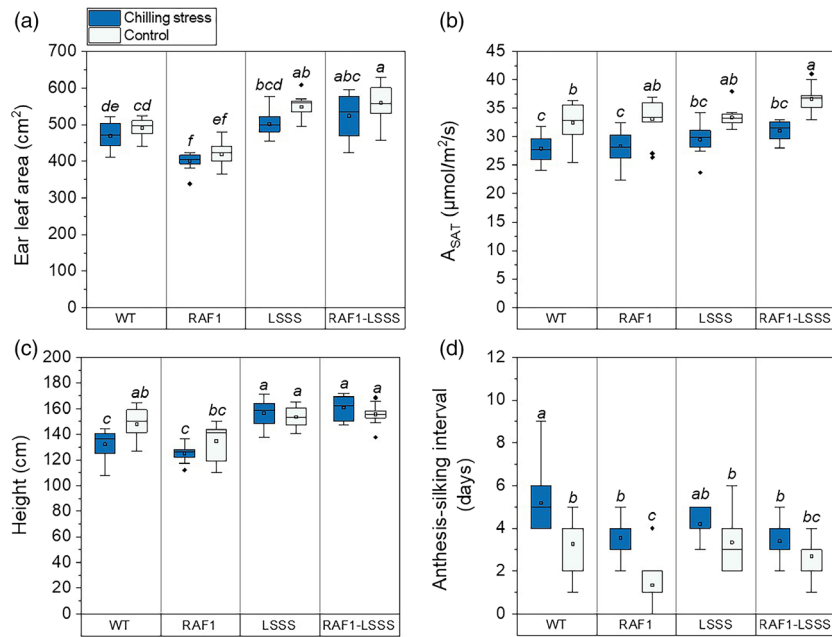
Table 2 Summary of leaf gas exchange and growth of full-grown maize plants (reproductive developmental stage) exposed to chilling stress early in development

Parameter		WT	RAF1	LSSS	RAF1-LSSS	Sample number (N)
Leaf gas exchange						
A_{SAT} (µmol/m^2/s)	Control	32.5 ± 1.1 b	33.1 ± 1.1 b	33.4 ± 0.66 ab	**36.6 ± 0.79 a**	9–11
	2 weeks of chilling	27.9 ± 0.72 b	28.3 ± 0.92 ab	29.5 ± 0.89 ab	**31.1 ± 0.53 a**	10–11
Growth traits						
Height (cm)	Control	147.8 ± 3.5 a	**134.7 ± 4.2 b**	152.7 ± 3.1 a	155.6 ± 2.7 a	9–11
	2 weeks of chilling	132.1 ± 3.5 b	125.1 ± 2.0 b	**156.5 ± 3.2 a**	**160.7 ± 3.0 a**	10–11
Ear Leaf Area (cm^2)	Control	491.3 ± 7.2 b	**419.1 ± 10.0 c**	**548.5 ± 11.7 a**	**560.2 ± 16.4 a**	9–11
	2 weeks of chilling	469.8 ± 11.2 b	**400.1 ± 7.1 c**	502.0 ± 11.3 ab	**523.6 ± 18.2 a**	10–11
Days to anthesis	Control	51.1 ± 0.34 a	51.2 ± 0.46 a	49.9 ± 0.40 ab	**48.7 ± 0.34 b**	9–11
	2 weeks of chilling	59.6 ± 0.34 a	59.4 ± 0.34 a	58.9 ± 0.28 ab	**57.7 ± 0.34 b**	10–11
Days to silking	Control	54.4 ± 0.58 a	52.7 ± 0.36 ab	53.0 ± 0.46 ab	**51.4 ± 0.34 b**	9–11
	2 weeks of chilling	64.8 ± 0.48 a	**62.9 ± 0.48 b**	63.1 ± 0.41 b	**61.1 ± 0.35 c**	10–11
Anthesis-silking interval (days)	Control	3.3 ± 0.43 a	**1.3 ± 0.41 b**	3.1 ± 0.48 a	2.7 ± 0.30 ab	9–11
	2 weeks of chilling	5.2 ± 0.44 a	**3.6 ± 0.28 b**	4.2 ± 0.25 ab	**3.4 ± 0.27 a**	9–11

Data represent averages ± SE. Statistical significance tests were conducted using one-way Tukey–Kramer HSD ANOVA. Values followed by the same letter are not significantly different at $P < 0.05$. Values significantly different from WT at $P < 0.05$ are in bold.

content does not limit photosynthetic rate during chilling. It is likely this difference is due to conditions under which the measurements were made. From these data sets, Rubisco appears to be most limiting under high/saturating light chilling conditions (gas exchange measurements) rather than medium to low light chilling conditions (chlorophyll fluorescence measurements). It is important to note, however, that although we saw an improvement in CO_2 assimilation under high light conditions, increased Rubisco was not enough to obtain anywhere near prestress photosynthetic rates, also suggesting that Rubisco is not the primary limiting factor of photosynthetic efficiency under chilling conditions. PPDK is another enzyme believed to limit CO_2 assimilation in C_4 plants, particularly under chilling conditions where it is prone to degradation (Du et al., 1999; Furbank et al., 1997). An alternative transgenic strategy to improve the photosynthetic rate in maize during chilling might be introduction of

Miscanthus × giganteus PPDK, whose abundance is stable during chilling (Naidu et al., 2003; Wang, Portis, et al., 2008). Additionally, identification of transcription factors that may be responsible for the differential gene expression observed between maize and Miscanthus during chilling could be the key in improving chilling tolerance of maize.

While results for RAF1-LSSS can be rationalized by increased Rubisco accumulation, LSSS presents more of an enigma, as increased CO_2 assimilation argues that overexpression of the Rubisco subunits can also be beneficial during chilling, even unaccompanied by additional holoenzyme accumulation. Chilling stress has been shown to decrease rbcL transcript levels in cucumber and RBCS transcript levels in both cucumber and maize (Riva-Roveda et al., 2016; Zhou et al., 2006), which the ubiquitin promoter-driven transgenes would mitigate in maize. Chilling can also enhance holoenzyme degradation, which is thought to be

due to reactive oxygen species that accumulate due to chilling stress-induced photoinhibition (Ishida *et al.*, 1999; Nakano *et al.*, 2006). For example, maize plants grown at 14 °C were shown to accumulate Rubisco breakdown products due to oxidative damage and proteolysis (Kingston-Smith et al., 1999; Kingston-Smith and Foyer, 2000). Overexpression of LSSS was previously shown to be beneficial under warm conditions, where it may be increasing the rate or efficiency of Rubisco assembly (Salesse-Smith *et al.*, 2018). It is likely that increases in subunit synthesis may be particularly beneficial during chilling, when Rubisco is susceptible to degradation. In addition, this benefit appears to outweigh any decreases in electron transport which may be caused by the energy invested in subunit overexpression.

Chilling early in development also proved to have lasting impacts as observed in fully grown plants (Figure 6). Flowering time (days to anthesis and silking) increased by ~10 days when plants were exposed to 2 weeks of chilling, likely due to reduced growth observed by decreased height and ear leaf area during the stress period (Table 1). This results in older plants with lower levels of photosynthesis during pollination, kernel development and grain filling, due to leaf aging and senescence (Crafts-Brandner and Poneleit, 1987). This could have negative effects on yield in maize, which mainly depends on postsilking photosynthetic rates (Chen *et al.*, 2015; Zhu *et al.*, 2010). Delayed sowing has been shown to limit the supply of assimilates during grain fill, leading to reduced yields (Bonelli *et al.*, 2016). RAF1-LSSS plants maintained significantly higher postsilking photosynthetic rates and a shorter flowering time compared to WT plants under both control and stressed conditions (Figure 6b, Table 1). This could potentially lead to improved yield relative to WT plants under both growth conditions in the field. Final height was significantly decreased in WT plants that had undergone chilling stress, but not in any of the transgenic lines. This demonstrates that not only does chilling stress delay growth during stress, but it can also reduce overall growth in more sensitive genotypes. In addition, the ASI of WT and RAF1 plants was significantly increased when exposed to chilling stress early in development, indicating asynchrony in flowering time. Increases in ASI occur in response to stress when ear growth slows in relation to tassel growth, which is hypothesized to be a response to the production of reduced levels of photosynthate. ASI has also been shown to be a good predictor of grain yield under stress, where increases in ASI are correlated with decreases in yield (Edmeades *et al.*, 2000). These results are another indication of a potential yield advantage for RAF1-LSSS, particularly in situations where chilling stress had been encountered.

In this study, we have demonstrated that increased Rubisco content appears to reduce the severity of chilling stress and allow for more rapid recovery; however, the photosynthetic rates of these plants were still significantly reduced when compared to control conditions. This finding indicates that the plants are not chilling tolerant and that chilling sensitivity in maize is likely due to a direct effect of temperature decreasing Calvin–Benson cycle activity rather than an indirect effect from photoinhibition of PSII. RAF1-LSSS plants show increased photosynthetic rates and growth before, during and after chilling stress when compared to WT. In addition, they showed no disadvantage when grown under heat stress conditions. These results provide new information on how Rubisco impacts chilling stress in maize which will be important for the field of crop biotechnology and for selecting alternative strategies and/or targets to manipulate and develop more chilling-tolerant maize plants.

Experimental procedures

Plant materials, growth conditions and measurements

Transgenic lines were described in Salesse-Smith *et al.* (2018). Plants were grown in 6L pots filled with 1/3 Metro-Mix® 360 (SunGro Horticulture) and 2/3 turface calcined clay soil mix. Plants were fertilized with Peters Excel® Cal-Mag 15-5-15 (ICL specialty fertilizers) at 200 ppm N every Monday, Wednesday and Friday until harvest. For growth chamber experiments (Figures 1–5), plants were grown in Conviron BDW40 units under 25 °C/16-h days and 20 °C/8-h nights at a light intensity of 350–400 µmol/m^2/s and relative humidity of 70%. Three weeks after planting, the plants underwent chilling for 2 weeks, 14 °C/16-h days and 12 °C/8-h nights. This was followed by 1 week of recovery under control conditions. For greenhouse experiments (Figure 6), plants were grown in chambers for 6 weeks, with or without chilling, transferred to the greenhouse and grown under natural illumination at 28/25 °C day/night until mature. Height was measured at the collar of the youngest fully expanded leaf, at the frequency indicated in the figures and tables. Stalk diameter was measured at its widest point. Leaf area was measured on the youngest fully expanded leaf or ear leaf of each plant under the condition specified as length × maximum width × A, where A is 0.75 (Francis *et al.*, 1969). Above-ground fresh weight was measured after cutting the plant just above the soil. Dry weight was measured after leaves and stems were dried at 40 °C for 2 weeks. Days to silking, anthesis and the derivate ASI (time to silking minus time to anthesis) were measured from the sowing date.

Leaf gas exchange

Gas exchange measurements were performed using the LI-6800-01A portable infrared gas analyzer (LI-COR Biosciences, Nebraska). Measurements were made on the youngest fully expanded leaves of 3-week-old (prestress), 5-week-old (2 weeks of chilling stress) and six-week-old (1-week recovery) plants. Responses of net CO_2 assimilation rate (A) to intercellular CO_2 concentration (Ci) were measured at a leaf temperature of 25 °C (prestress and recovery) or 14 °C (chilling stress), and a light intensity of 1800 µmol/m^2/s. Plants were acclimated to these conditions until steady-state gas exchange was reached (20–30 min), and A/Ci curves measured with a sequence of reference CO_2 concentrations of 400, 300, 250, 200, 150, 100, 75, 50, 400, 400, 400, 400, 500, 600, 800, 1000 and 1200 µmol/mol. The middle four measurements at 400 µmol/mol were disregarded, as their purpose was to allow the plant to re-acclimate to this condition after being exposed to low CO_2 concentrations. Data points were taken in sequential order with an equilibration time of 180–300 s at each CO_2 concentration. In the greenhouse experiment, A_{SAT} was measured on the ear leaf the day silks emerged, at a CO_2 concentration of 400 µmol/mol, a leaf temperature of 25 °C, and a light intensity of 1800 µmol/m^2/s.

Chlorophyll fluorescence

Chlorophyll fluorescence measurements were performed using the LI-6800-01A Pulse Amplitude Modulated (PAM) multiphase flash fluorometer on the plant materials described above for *A-C$_i$* curves, at a CO_2 concentration of 400 µmol/mol and a light intensity of 360 µmol/m^2/s (the ambient light intensity in the growth chamber the day measurements were made). F_v/F_m was calculated as $(F_m–F_o)/F_m$, where F_m is the maximum fluorescence

level after a saturating pulse and F_o is the minimum fluorescence level of the dark-adapted plant. For F_v/F_m measurements, plants were dark adapted for at least 30 min. Φ_{II} was calculated as $(F'_m - F'_s)/F'_m$ (Genty *et al.*, 1989), where F'_m is the maximum fluorescence level from a light-adapted plant after a saturating pulse and F_s is the steady-state fluorescence level under actinic light. *NPQ* was calculated as $(F_m - F'_m)/F'_m$ (Bilger and Björkman, 1990) and q_L as $(F'_o/F_s)(F'_m - F_s)/(F'_m - F'_o)$, where F'_o is the minimum fluorescence level of a light-acclimated plant, measured after a short exposure to far-red light (Kramer *et al.*, 2004). The energy partitioning of light-acclimated plants in the absence of actinic light was calculated following the approach of Kornyeyev and Holaday (2008), as modified by Busch *et al.* (2009):

$$\Phi_{PSII} = \frac{F'_v}{F'_m} = \frac{F'_m - F'_o}{F'_m}$$

$$\Phi_{REG} = 1 - \frac{F'_v}{F'_m} / \frac{F_v}{F_m}$$

$$\Phi_{CI} = \left(1 - \frac{F_v}{F_m} / \frac{F_{vM}}{F_{mM}}\right)\left(\frac{F'_v}{F'_m} / \frac{F_v}{F_m}\right),$$

and

$$\Phi_{f,CON} = 1 - \Phi_{PSII} - \Phi_{REG} - \Phi_{CI} = \left(1 - \frac{F_{vM}}{F_{mM}}\right)\left(\frac{F'_v}{F'_m} / \frac{F_{vM}}{F_{mM}}\right),$$

where F_{vM}/F_{mM} is the fully relaxed optimum quantum efficiency of PSII measured on unstressed plants. Here, we used the value of measured under control conditions at 25 °C before the plants were exposed to chilling stress.

Enzyme activity, activation and protein analysis

Following gas exchange measurements under chilling stress conditions, replicate leaf samples (0.5 cm^2) were frozen in liquid nitrogen and stored at −80 °C. Soluble protein was subsequently extracted from each leaf disc using 800 μL of extraction buffer, and Rubisco activity, activation state and protein content were measured exactly as described in Salesse-Smith *et al.* (2018). For immunoblotting, total protein was extracted on a leaf area basis from the tip of the youngest fully developed leaf prestress (control) or after 2 weeks of chilling stress, as described in Barkan (1998). Proteins were separated, transferred and detected as described in Salesse-Smith *et al.* (2018). The following primary antibodies were used at a dilution of 1:10 000: anti-LS (Agrisera), anti-PPDK (Agrisera) and anti-RAF1 (Feiz *et al.*, 2012). RCA protein was quantified using the Odyssey infrared imager and Image Studio Lite software (Li-Cor Biosciences).

Statistical analysis

The effects of chilling stress were analysed using a one-way ANOVA with a post hoc Tukey HSD tests for pairwise comparisons of the means. Values with $P < 0.05$ were considered significantly different, where different lowercase letters indicate significant differences. Jmp pro version 13.1.0 software and OriginPro 2019 were used for all statistical analyses.

Conflict of Interest

The authors declare no conflict of interest.

Author Contributions

CS participated in all experiments and drafted the manuscript; RES participated in experiments shown in Figures 3, 5, S2 and Table 1; FAB participated in experiments shown in Figure 3, 4, S2 and Table 1; DBS was responsible for project management and finalization of data analysis and manuscript preparation.

References

Allen, D.J. and Ort, D.R. (2001) Impacts of chilling temperatures on photosynthesis in warm-climate plants. *Trends Plant Sci.* **6**, 36–42.

Andrews, J.R., Fryer, M.J. and Baker, N.R. (1995) Characterization of chilling effects on photosynthetic performance of maize crops during early season growth using chlorophyll fluorescence. *J. Exp. Bot.* **46**, 1195–1203.

Beale, C.V., Bint, D.A. and Long, S.P. (1996) Leaf photosynthesis in the C4-grass Miscanthus x giganteus, growing in the cool temperate climate of southern England. *J. Exp. Bot.* **47**, 267–273.

Bilger, W. and Björkman, O. (1990) Role of the xanthophyll cycle in photoprotection elucidated by measurements of light-induced absorbance changes, fluorescence and photosynthesis in leaves of *Hedera canariensis*. *Photosynth Res* **25**, 173–185.

Bonelli, L.E., Monzon, J.P., Cerrudo, A., Rizzalli, R.H. and Andrade, F.H. (2016) Maize grain yield components and source-sink relationship as affected by the delay in sowing date. *Field. Crop. Res.* **198**, 215–225.

Busch, F., Hüner, N.P.A. and Ensminger, I. (2009) Biochemical constrains limit the potential of the photochemical reflectance index as a predictor of effective quantum efficiency of photosynthesis during the winter spring transition in Jack pine seedlings. *Functional Plant Biol.* **36**, 1016.

von Caemmerer, S. (2000) *Biochemical Models of Leaf Photosynthesis*. Clayton, Australia: CSIRO Publishing.

Chen, Y., Xiao, C., Wu, D., Xia, T., Chen, Q., Chen, F. *et al.* (2015) Effects of nitrogen application rate on grain yield and grain nitrogen concentration in two maize hybrids with contrasting nitrogen remobilization efficiency. *Eur. J. Agron.* **62**, 79–89.

Crafts-Brandner, S.J. and Poneleit, C.G. (1987) Effect of ear removal on CO(2) exchange and activities of ribulose bisphosphate carboxylase/oxygenase and phosphoenolpyruvate carboxylase of maize hybrids and inbred lines. *Plant Physiol.* **84**, 261–265.

Dohleman, F.G. and Long, S.P. (2009) More productive than maize in the midwest: how does miscanthus do it? *Plant Physiol.* **150**, 2104–2115.

Du, Y.-C., Nose, A. and Wasano, K. (1999) Thermal characteristics of C4 photosynthetic enzymes from leaves of three sugarcane species differing in cold sensitivity. *Plant Cell Physiol.* **40**, 298–304.

Edmeades, G.O., Bolaños, J., Elings, A., Ribaut, J.-M., Bänziger, M. and Westgate, M.E. (2000) The role and regulation of the anthesis-silking interval in maize. *Physiol. Model. Kernel Set in Maize*, **29**, 43–73.

Ehleringer, J. and Björkman, O. (1977) Quantum yields for CO$_2$ uptake in C3 and C4 plants: dependence on temperature, CO$_2$, and O$_2$ concentration. *Plant Physiol.* **59**, 86–90.

Farage, P.K., Blowers, D., Long, S.P. and Baker, N.R. (2005) Low growth temperatures modify the efficiency of light use by photosystem II for CO$_2$ assimilation in leaves of two chilling-tolerant C4 species, Cyperus longus L. and Miscanthus × giganteus. *Plant, Cell Environ.* **29**, 720–728.

Feiz, L., Williams-Carrier, R., Wostrikoff, K., Belcher, S., Barkan, A. and Stern, D.B. (2012) Ribulose-1,5-bis-phosphate carboxylase/oxygenase accumulation factor1 is required for holoenzyme assembly in maize. *Plant Cell*, **24**, 3435–3446.

Francis, C.A., Rutger, J.N. and Palmer, A.F.E. (1969) A rapid method for plant leaf area estimation in maize (Zea mays L.) 1. Crop Sci. **9**, 537–539.

Friesen, P.C. and Sage, R.F. (2016) Photosynthetic responses to chilling in a chilling-tolerant and chilling-sensitive Miscanthus hybrid. Plant, Cell Environ. **39**, 1420–1431.

Fryer, M.J., Oxborough, K., Martin, B., Ort, D.R. and Baker, N.R. (1995) Factors associated with depression of photosynthetic quantum efficiency in maize at low growth temperature. Plant Physiol. **108**, 761–767.

Furbank, R.T., Chitty, J.A., Jenkins, C.L.D., Taylor, W.C., Trevanion, S.J., von Caemmerer, S. and Ashton, A.R. (1997) Genetic manipulation of key photosynthetic enzymes in the C4 plant Flaveria bidentis. Functional Plant Biol. **24**, 477–485.

Genty, B., Briantais, J.-M. and Baker, N.R. (1989) The relationship between the quantum yield of photosynthetic electron transport and quenching of chlorophyll fluorescence. Biochem. Biophys. Acta. **990**, 87–92.

Ishida, H., Makino, A. and Mae, T. (1999) Fragmentation of the large subunit of ribulose-1,5-bisphosphate carboxylase by reactive oxygen species occurs near gly-329. J. Biol. Chem. **274**, 5222–5226.

Kingston-Smith, A.H. and Foyer, C.H. (2000) Bundle sheath proteins are more sensitive to oxidative damage than those of the mesophyll in maize leaves exposed to paraquat or low temperatures. J. Exp. Bot. **51**, 123–130.

Kingston-Smith, A.H., Harbinson, J. and Foyer, C.H. (1999) Acclimation of photosynthesis, H2O2 content and antioxidants in maize (Zea mays) grown at sub-optimal temperatures. Plant, Cell Environ. **22**, 1071–1083.

Kornyeyev, D. and Holaday, A.S. (2008) Corrections to current approaches used to calculate energy partitioning in photosystem 2. Photosynthetica, **46**, 170–178.

Kramer, D.M., Johnson, G., Kiirats, O. and Edwards, G.E. (2004) New fluorescence parameters for the determination of Q_A redox state and excitation energy fluxes. Photosynth. Res. **79**, 209–218.

Kromdijk, J., Głowacka, K., Leonelli, L., Gabilly, S.T., Iwai, M., Niyogi, K.K. and Long, S.P. (2016) Improving photosynthesis and crop productivity by accelerating recovery from photoprotection. Science, **354**, 857–861.

Kubien, D.S., von Caemmerer, S., Furbank, R.T. and Sage, R.F. (2003) C4 Photosynthesis at low temperature. A study using transgenic plants with reduced amounts of Rubisco. Plant Physiol. **132**, 1577–1585.

Long, S.P. (1983) C4 photosynthesis at low temperatures. Plant, Cell Environ. **6**, 345–363.

Long, S.P. (1999) Environmental responses. In: C4 plant biology (Sage, R.F. and Monson, R.K. eds.), pp. 215–249. San Diego, CA: Academic Press.

Long, S.P. and Spence, A.K. (2013) Toward cool C4 crops. Annu. Rev. Plant Biol. **64**, 701–722.

Long, S.P., Humphries, S. and Falkowski, P.G. (1994) Photoinhibition of photosynthesis in nature. Annu. Rev. Plant Physiol. Plant Mol. Biol. **45**, 633–662.

Maxwell, K. and Johnson, G.N. (2000) Chlorophyll fluorescence—a practical guide. J. Exp. Bot. **51**, 659–668.

Munekage, Y., Hojo, M., Meurer, J., Endo, T., Tasaka, M. and Shikanai, T. (2002) PGR5 is involved in cyclic electron flow around photosystem I and is essential for photoprotection in Arabidopsis. Cell, **110**, 361–371.

Murchie, E.H. and Lawson, T. (2013) Chlorophyll fluorescence analysis: a guide to good practice and understanding some new applications. J. Exp. Bot. **64**, 3983–3998.

Naidu, S.L. and Long, S.P. (2004) Potential mechanisms of low-temperature tolerance of C4 photosynthesis in Miscanthus × giganteus: an in vivo analysis. Planta, **220**, 145–155.

Naidu, S.L., Moose, S.P., AL-Shoaibi, A.K., Raines, C.A., and Long, S.P. (2003) Cold tolerance of C4 photosynthesis in Miscanthus × giganteus: adaptation in amounts and sequence of C4 photosynthetic enzymes. Plant Physiol. **132**, 1688–1697.

Nakano, R., Ishida, H., Makino, A. and Mae, T. (2006) In vivo fragmentation of the large subunit of ribulose-1,5-bisphosphate carboxylase by reactive oxygen species in an intact leaf of cucumber under chilling-light conditions. Plant Cell Physiol. **47**, 270–276.

Osborne, C.P., Wythe, E.J., Ibrahim, D.G., Gilbert, M.E. and Ripley, B.S. (2007) Low temperature effects on leaf physiology and survivorship in the C3 and C4 subspecies of Alloteropsis semialata. J. Exp. Bot. **59**, 1743–1754.

Ranum, P., Peña-Rosas, J.P. and Garcia-Casal, M.N. (2014) Global maize production, utilization, and consumption. Ann. N. Y. Acad. Sci. **1312**, 105–112.

Riva-Roveda, L., Escale, B., Giauffret, C. and Périlleux, C. (2016) Maize plants can enter a standby mode to cope with chilling stress. BMC Plant Biol. **16**, 212. https://doi.org/10.1186/s12870-016-0909-y

Ruelland, E., Vaultier, M.-N., Zachowski, A. and Hurry, V. (2009) Chapter 2 cold signalling and cold acclimation in plants. In Advances in Botanical Research, Vol. **49** (Kader, J.-C. and Delseny, M., eds), pp. 35–150. Cambridge, MA: Academic Press.

Sage, R.F. (2002) Variation in the k_cat of Rubisco in C3 and C4 plants and some implications for photosynthetic performance at high and low temperature. J. Exp. Bot. **53**, 609–620.

Sage, R.F., Pearcy, R.W. and Seemann, J.R. (1987) The nitrogen use efficiency of C3 and C4 Plants: III. Leaf nitrogen effects on the activity of carboxylating enzymes in Chenopodium album (L.) and Amaranthus retroflexus (L.). Plant Physiol. **85**, 355–359.

Sage, R.F., Sage, T.L. and Kocacinar, F. (2012) Photorespiration and the evolution of C4 photosynthesis. Annu. Rev. Plant Biol. **63**, 19–47.

Salesse-Smith, C.E., Sharwood, R.E., Busch, F.A., Kromdijk, J., Bardal, V. and Stern, D.B. (2018) Overexpression of Rubisco subunits with RAF1 increases Rubisco content in maize. Nat. Plants, **4**, 802.

Salvucci, M.E., Osteryoung, K.W., Crafts-Brandner, S.J. and Vierling, E. (2001) Exceptional sensitivity of Rubisco activase to thermal denaturation in vitro and in vivo. Plant Physiol. **127**, 1053–1064. https://doi.org/10.1104/pp.010357

Sharwood, R.E., Ghannoum, O. and Whitney, S.M. (2016) Prospects for improving CO2 fixation in C3-crops through understanding C4-Rubisco biogenesis and catalytic diversity. Curr. Opin. Plant Biol. **31**, 135–142.

Smillie, R.M. and Hetherington, S.E. (1983) Stress tolerance and stress-induced injury in crop plants measured by chlorophyll fluorescence in vivo: chilling, freezing, ice cover, heat, and high light. Plant Physiol. **72**, 1043–1050.

Spence, A.K., Boddu, J., Wang, D., James, B., Swaminathan, K., Moose, S.P. and Long, S.P. (2014) Transcriptional responses indicate maintenance of photosynthetic proteins as key to the exceptional chilling tolerance of C4 photosynthesis in Miscanthus × giganteus. J. Exp. Bot. **65**, 3737–3747.

Wang, D., Naidu, S.L., Portis, A.R., Moose, S.P. and Long, S.P. (2008) Can the cold tolerance of C4 photosynthesis in Miscanthus×giganteus relative to Zea mays be explained by differences in activities and thermal properties of Rubisco? J. Exp. Bot. **59**, 1779–1787.

Wang, D., Portis, A.R., Moose, S.P. and Long, S.P. (2008) Cool C4 photosynthesis: pyruvate Pi dikinase expression and activity corresponds to the exceptional cold tolerance of carbon assimilation in Miscanthus × giganteus. Plant Physiol. **148**, 557–567.

Wostrikoff, K., Clark, A., Sato, S., Clemente, T. and Stern, D. (2012) Ectopic expression of Rubisco subunits in maize mesophyll cells does not overcome barriers to cell type-specific accumulation. Plant Physiol. **160**, 419–432.

Zhou, Y.-H., Yu, J.-Q., Mao, W.-H., Huang, L.-F., Song, X.-S. and Nogués, S. (2006) Genotypic variation of Rubisco expression, photosynthetic electron flow and antioxidant metabolism in the chloroplasts of chill-exposed cucumber plants. Plant Cell Physiol. **47**, 192–199.

Zhu, X.-G., Long, S.P. and Ort, D.R. (2010) Improving photosynthetic efficiency for greater yield. Annu Rev. Plant Biol. **61**, 235–261.

Supporting information

Additional supporting information may be found online in the Supporting Information section at the end of the article.

Figure S1 Growth of transgenic plants after 2 weeks of chilling stress and one week of recovery.

Figure S2 A/Ci response curves measured on the youngest fully expanded leaves of 5-week-old plants exposed to chilling stress for 2 weeks, grown under high light (600 μmol/m^2/s).

Figure S3 Effect of chilling stress on chlorophyll fluorescence parameters.

Figure S4 Immunoblot analysis of proteins before and after 2 weeks of chilling stress at 14 °C.

Figure S5 Impact of chilling stress on growth rate.

Figure S6 Effect of short-term heat stress (40 °C for 48 h).